# Automated deep learning-based segmentation of brain, SEEG and DBS electrodes on CT images

Vanja Vlasov[1], Marie Bofferding[2], Loïc Marx[1], Chencheng Zhang[3], Jorge Goncalves[1], Andreas Husch[1], Frank Hertel[1,4]

[1]Luxembourg Centre for Systems Biomedicine (LCSB), University of Luxembourg, Belvaux, Luxembourg
[2]Otto von Guericke University Magdeburg, Germany
[3]Department of Functional Neurosurgery, Ruijin Hospital, Shanghai Jiao Tong University School of Medicine, Shanghai, China
[4]National department of Neurosurgery, Hospital Centre of Luxembourg (CHL), Luxembourg
vanja.vlasov@uni.lu

**Abstract.** Stereoelectroencephalography (sEEG) and deep brain stimulation (DBS) are effective surgical diagnostic and therapeutic procedures of the depth electrodes implantation in the brain. The benefit and outcome of these procedures directly depend on the electrode placement. Our goal was to accurately segment and visualize electrode position after the sEEG and DBS procedures. We trained a deep learning network to automatically segment electrodes trajectories and brain tissue from postsurgical CT images. We used 90 head CT scans that include intracerebral electrodes and their corresponding segmentation masks to train, validate and test the model. Mean accuracy and dice score in 5-fold cross-validation for the 3D-cascade U-Net model were 0.99 and 0.92, respectively. When the network was tested on an unseen test set, the dice overlap with the manual segmentations was 0.89. In this paper, we present a deep-learning approach for automatic patient-specific delineation of the brain, the sEEG and DBS electrodes from different varying quality of CT images. This robust method may inform on the postsurgical electrode positions fast and accurately. Moreover, it is useful as an input for neurosurgical and neuroscientific toolboxes and frameworks.

## 1 Introduction

With advances in stereotactic techniques, robotics and neuroimaging, there has been a worldwide increase in the use of stereoelectroencephalography (sEEG)[1]. SEEG is a surgical diagnostic procedure that helps to find brain areas responsible for the epileptogenic activity in the complex cases of epilepsy. During the sEEG surgery, 4 to 18 depth electrodes are implanted in the patient's brain to record local field potentials from several brain structures. Depth electrode recordings are sampled from the electrode entry site along the trajectory to the final target

point. Therefore, fast and accurate 3D visualization of the implanted electrodes is crucial for the outcome of the procedure and the following therapeutic decision.

Automated, accurate deep brain stimulation (DBS) electrode delineations toolboxes have been used in neurosurgical and scientific practice[2,3]. However, there is a lack of available, successful tools for sEEG electrode segmentation and state-of-the-art in postsurgical electrode evaluation is still done visually by clinicians. This approach is based on the co-registration of patient image modalities, it is prone to errors and time-consuming. Due to extensive metal artefacts, electrodes thin nature, banding and overlapping, the simple thresholding of appropriate Hounsfield units is not satisfactory to segment implanted electrodes from a CT volume. Recently published semi-automated toolboxes for sEEG segmentation are an improvement of the state-of-the-art, but not validated on a larger heterogeneous data-sets [4,5,6,7]. Arnulfo et al. segment sEEG contacts from a thresholded cone-beam homogeneous voxel space CT images based on presurgical planned trajectories[4]. However, the error might arise with this approach since sEEG electrodes are bending and overlapping and their postoperative trajectories are not as planned before the surgery. Novel methods are also mostly based on patient MRI and CT co-registration and not on deep learning[5,6]. These methods require manual corrections and annotations when patients unilateral or bilateral electrodes are overlapping.

Novel advances in deep learning provided frameworks for training a convolutional neural network (CNN) specialized for medical imaging[8]. We trained such a network in order to develop a robust, automated and a fast electrode and brain segmentation tool for CT imaging. Our solution is not requiring any additional imaging modality and preprocessing. By including post-operative DBS imaging, we increase a dataset and ensure to learn a solution that is robust towards all kinds of depth electrodes.

## 2 Materials and methods

### 2.1 Dataset description

A total of 90 anonymised head CT image data set from patients that underwent routine clinical planning of stereotactic surgery procedures was available for this study. The data set contained post-operative CT imaging with one or more electrodes implanted in the brain as part of a DBS or SEEG procedure and additional pre-operative T1- weighted MRIs. Post-DBS scans were acquired at the Centre Hospitalier de Luxembourg (40 images, 81 DBS electrodes) and post-sEEG scans at the Shanghai Rujin Hospital (50 images, 334 sEEG electrodes). Among the data-set were CT images obtained in different centres using three CT scanner vendors, images of different quality and reconstructed with other than soft-tissue filters, for example, bone-filter CT scans. Images with implant- and patient-based artifacts, such as beam hardening and metal or motion artifacts, were included in the study. For training the network, 35 post DBS and 45 post sEEG CT volumes were randomly selected. The remaining 10 CT images were

used as a network performance test set. To generate CT image labels for training, firstly, the brain was extracted and DBS electrodes were segmented with a previously published pipeline [2]. Secondly, across the post sEEG CT scans the fitting high Hounsfield Unit (HU) intensity threshold was used to extract all the electrodes and wires. Finally, all electrodes and brain labels in CT space were manually corrected and unnecessary wires and bone structures were removed using ITK-SNAP.

The training data was split into five random cross-validation sets. Training CT images and corresponding labels were resampled to the median voxel dimension of the image volumes, $0.48 \times 0.48 \times 0.66mm$.

### 2.2 Network architecture

As CT volumes are impractical and memory expensive to train the full 3D resolution, with the input size of $512 \times 512 \times X$ , the 3D-cascade U-net model enables the network to accumulate contextual and spatial information. The 3D cascade U-net model architecture, used in this work for segmentation, has been designed from the nnU-Net framework[8]. The architecture of the network is

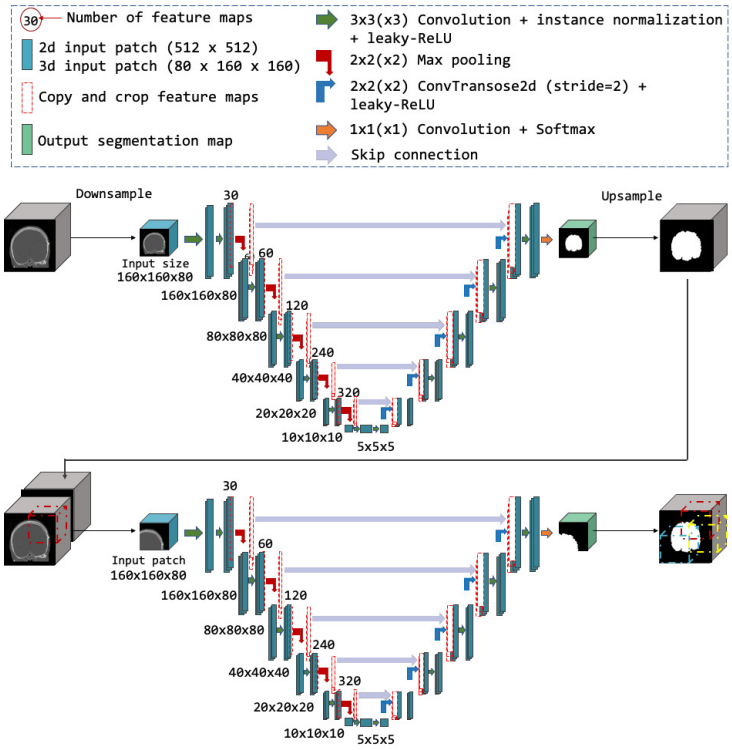


**Fig. 1.** Two parts of the 3D Cascade U-Net model network architecture: low resolution 3D U-Net following with patch based 3D U-Net.

shown in Fig. 1., where first a 3D-low-resolution U-net is employed followed by a full high-resolution 3D U-net on smaller image patches. Random rotations and translations were used to augment the training data.

The framework utilizes a loss-function combining dice-loss and cross-entropy loss to mitigate class imbalance problems. The initial learning rate of the stochastic gradient descent was $10^{-2}$ with a decay of $3 \times 10^{-5}$. Learning was terminated due to no further improvement of the validation loss.

Data processing was carried out on the High-Performance-Computing (HPC) cluster of the University of Luxembourg, utilizing four Tesla V100 GPU with 16GB GPU Memory.

### 2.3 Performance assessment

In addition to the cross-validation, we evaluated the trained network on the independent test set. Within the test set, there was a CT scan with a bone reconstruction kernel instead of the typical soft tissue filter allowing insights on performance on different CT reconstruction noise. The segmentation performance was assessed using the Sørensen-Dice similarity coefficient.

## 3 Results

The mean accuracy for the model in the cross-validation was $> 0.99$ and mean Dice Coefficient was 0.921. In the analysis on the independent test set, comparing network segmentation of both brain and electrodes label with manual segmentation, the mean dice score with standard deviation was $0.897 \pm 0.043$ and average computation time of $230.2 \pm 65.4$ seconds.

Figure 2 illustrates the qualitative visualisation of the method segmentations. Segmentation's are shown for post-operative CT scans with implanted DBS and SEEG electrodes. Figure 3 shows an example of the network performance for CT image with bone reconstruction filter. Our U-Net achieved plausible segmentations in postsurgical images for both procedures. The nnU-net-based 3D Cascade model showed convincing performance. Furthermore, our method correctly labelled brain shift observed in frontal areas as background class.

## 4 Discussion

This paper introduced a nnU-net-based approach for depth electrode and brain segmentation from CT head scans.

One of the main concerns regarding using deep learning is a lack of generalisation: a network losing the ability to yield satisfactory results on input data with different properties than the training data. By including training data from two centres, different image quality and reconstruction filters, as well as the brain with SEEG and DBS electrode implants our network was able to learn to appropriately segment electrodes trajectories within and outside the brain

parenchyma. Moreover, our network delineated the sEEG electrodes and brain in very bad soft tissue contrast example in CT scan reconstructed with the bone kernel.

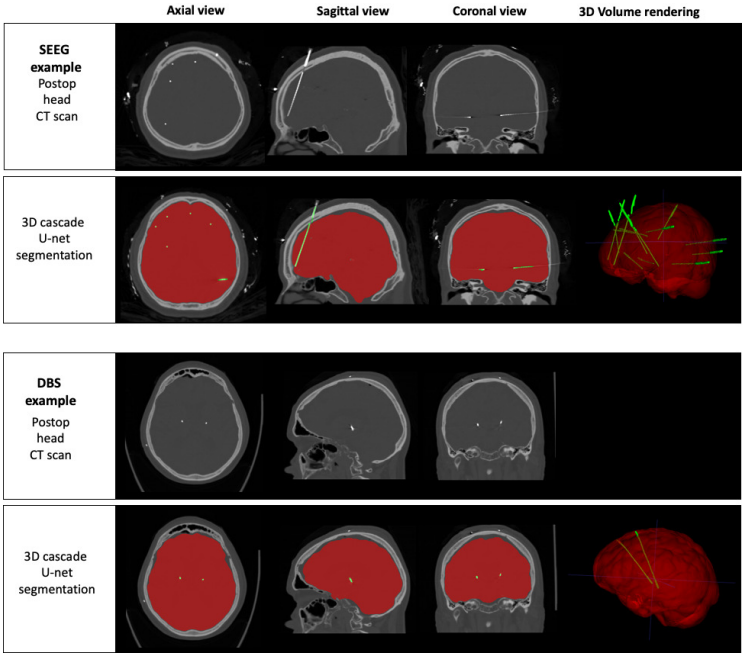


**Fig. 2.** Electrode and brain segmentation results of CT postsurgical imaging visualized in synchronized axial, sagittal, coronal planes and 3D patient specific surface rendered partly transparent volume. The extracted brain mask is presented in red and segmented electrodes in green.

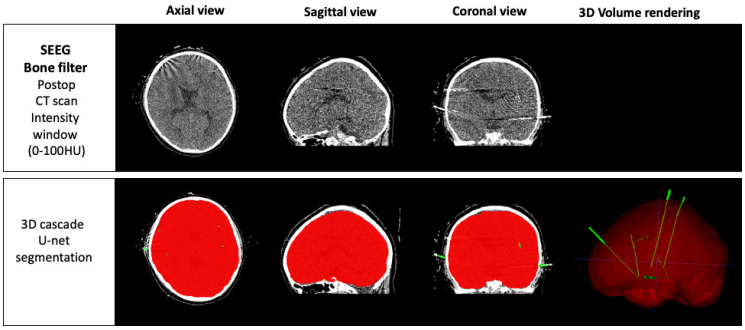


**Fig. 3.** Visual representation of the post-op head CT scan reconstructed using bone filter and electrode and brain segmentations obtained our network. The extracted brain mask is presented in red and segmented electrodes in green.

To our knowledge, this is the first deep-learning automated network that can robustly segment patient-specific depth electrodes after sEEG and DBS procedures and brain from CT scans. Our approach may inform on the postsurgical electrode contacts positions fast and accurate and be an input for neurosurgical and neuroscientific toolboxes and frameworks.

## 5 Acknowledgement

The experiments presented in this paper were carried out using the HPC facilities of the University of Luxembourg (Varrette, Bouvry, Cartiaux, & Georgatos, 2014) – see https://hpc.uni.lu.

We thank Dr. Krasimir Minkin and the Department of Neurosurgery, University Hospital "Saint Ivan Rilski", Sofia, Bulgaria, for providing single anonymised postsurgical sEEG CT volume for testing here presented models.

## References

1. Katz JS, Abel TJ. Stereoelectroencephalography Versus Subdural Electrodes for Localization of the Epileptogenic Zone: What Is the Evidence? Neurotherapeutics. 2019;16(1):59–66.
2. Husch A, Petersen MV, Gemmar P, et al. Post-operative deep brain stimulation assessment: Automatic data integration and report generation. Brain Stimul. 2018;11(4):863–866. Available from: https://doi.org/10.1016/j.brs.2018.01.031.
3. Horn A, Li N, Dembek TA, et al. Lead-DBS v2: Towards a comprehensive pipeline for deep brain stimulation imaging. NeuroImage. 2019 jan;184:293–316.
4. Arnulfo G, Narizzano M, Cardinale F, et al. Automatic segmentation of deep intracerebral electrodes in computed tomography scans. BMC Bioinformatics. 2015;16(1):1–12.
5. Blenkmann AO, Phillips HN, Princich JP, et al. Ielectrodes: A comprehensive open-source toolbox for depth and subdural grid electrode localization. Front Neuroinform. 2017;11(March):1–16.
6. Granados A, Vakharia V, Rodionov R, et al. Automatic segmentation of stereoelectroencephalography (SEEG) electrodes post-implantation considering bending. Int J Comput Assist Radiol Surg. 2018;13(6):935–946. Available from: https://doi.org/10.1007/s11548-018-1740-8.
7. Narizzano M, Arnulfo G, Ricci S, et al. SEEG assistant: A 3DSlicer extension to support epilepsy surgery. BMC Bioinformatics. 2017;18(1):1–13.
8. Isensee F, Petersen J, Klein A, et al. nnU-Net: Self-adapting Framework for U-Net-Based Medical Image Segmentation. Informatik aktuell. 2019; p. 22.